

Transversal flexoelectric coefficients for fifty select atomic monolayers from first principles

Shashikant Kumar,[†] David Codony,[‡] Irene Arias,^{‡,¶} and Phanish

Suryanarayana^{*,†}

[†]*College of Engineering, Georgia Institute of Technology, Atlanta, GA 30332, USA*

[‡]*Laboratori de Càlcul Numèric, Universitat Politècnica de Catalunya, Barcelona, E-08034, Spain*

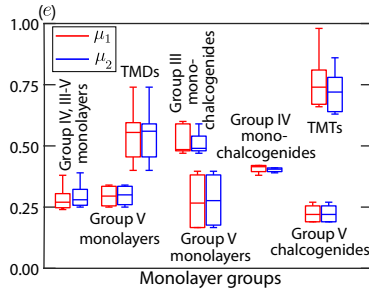
[¶]*Centre Internacional de Metodes Numèrics en Enginyeria (CIMNE), 08034 Barcelona, Spain*

E-mail: phanish.suryanarayana@ce.gatech.edu

Abstract

We calculate transversal flexoelectric coefficients along the principal directions for fifty select atomic monolayers using ab initio Density Functional Theory (DFT). Specifically, considering representative materials from each of Groups IV, III-V, V monolayers, transition metal dichalcogenides (TMDs), Group III monochalcogenides, Group IV monochalcogenides, transition metal trichalcogenides (TMTs), and Group V chalcogenides, we perform symmetry-adapted DFT simulations to calculate the flexoelectric coefficients at practically relevant bending curvatures. We find that the materials demonstrate linear behavior and have similar coefficients along both principal directions, with values for TMTs being up to a factor of five larger than graphene. In addition, we find electronic origins for the flexoelectric effect, which increases with monolayer thickness, elastic modulus along bending direction, and sum of polarizability of constituent atoms.

Graphical TOC Entry



Keywords

Flexoelectric effect, Density Functional Theory, Two-dimensional materials, Electromechanical coupling, Dipole moment, Strain gradient

Flexoelectricity¹⁻⁸ is an electromechanical property common to semiconductors/insulators that represents a two-way coupling between strain gradients and polarization. Unlike piezoelectricity, it is not restricted to materials that are non-centrosymmetric, i.e., lattice structures that do not possess inversion symmetry, and in contrast to electrostriction, it permits reversal of the strain by reversal of the electric field and allows for sensing in addition to actuation. Though the flexoelectric effect is generally negligible for bulk systems, it becomes significant in nanostructures/nanomaterials due to the possibility of extremely large strain gradients, especially along the directions in which the system has dimensions at the nanoscale.

The flexoelectric effect in two-dimensional materials has a number of applications — analogous to those found for other such electromechanical couplings⁹⁻¹³ — including sensors, actuators, and energy harvestors in nanoelectromechanical systems. Even in applications where the flexoelectric effect is not being exploited, e.g., flexible electronics,¹⁴⁻¹⁷ nanoelectromechanical devices,¹⁸⁻²¹ and nanocomposites,^{22,23} the presence of strain gradients such as those encountered during bending — a common mode of deformation in two-dimensional materials, given their relatively low bending moduli values²⁴ — makes flexoelectricity an important design consideration.^{25,26} This is evidenced by recent work where flexoelectricity has been shown to produce incorrect measurements of piezoelectric coefficients at the nanoscale.²⁷

Atomic monolayers, which are two-dimensional materials consisting of a single layer of material, have been the subject of intensive research over the past two decades,²⁸⁻³⁰ with dozens of monolayers having now been synthesized³¹⁻³⁶ and the potential for thousands more as predicted by ab initio calculations.^{37,38} The widespread interest in these systems is a consequence of their novel and exciting properties,^{31,32,34,35,39-42} which makes them ideal candidates for the aforementioned applications. However, the transversal flexoelectric coefficients for atomic monolayers — the relevant component of the flexoelectric tensor in the context of bending deformations — are far from being established.

Experimental data for the transversal flexoelectric coefficients of atomic monolayers is highly sparse, likely due to the challenges associated with isolating the flexoelectric and piezoelectric contributions.⁴³ Recently, the coefficients for some TMDs (MX_2 : $\text{M}=\text{Mo},\text{W}$; $\text{X}=\text{S},\text{Se}$) have been measured,^{43,44} however there is significant uncertainty in the results, due to large error bars and the use of substrates. On the theoretical side, studies based on ab initio Kohn-Sham DFT^{45,46} have been used to calculate the flexoelectric coefficients of graphene^{4,47-49} and some TMDs (MX_2 : $\text{M}=\text{Mo},\text{W}$; $\text{X}=\text{S},\text{Se},\text{Te}$).⁴⁹ However, as shown in recent work,⁵⁰ the accuracy of these results is limited by the use of an ill defined flexoelectric coefficient,^{48,49} artificial partitioning of the electron density,^{47,51} and/or geometries with non-uniform strain gradients.⁴⁹ Note that a theoretically more involved alternative is provided by density-functional perturbation theory (DFPT)^{52,53} — found to have significant success in the study of bulk like three-dimensional systems⁵⁴⁻⁵⁹ — which has very recently been extended to the study of two-dimensional systems.⁶⁰ Other theoretical efforts include the use of force fields,^{61,62} which differ by more than an order of magnitude from experimental/DFT results, suggesting that they are unsuitable in the current context.

In this work, using a recently developed formulation for the accurate computation of the transversal flexoelectric coefficient at finite deformations,⁵⁰ we perform a comprehensive first principles DFT study for the coefficients of fifty select atomic monolayers along their principal directions at practically relevant bending curvatures.⁶³⁻⁶⁶ We also provide fundamental insights into the flexoelectric effect for atomic monolayers and the variation in the coefficient values between them.

The transversal flexoelectric coefficient at finite bending deformations is defined as:⁵⁰

$$\mu = \frac{\partial p_r}{\partial \kappa}, \quad (1)$$

where p_r is the *radial polarization* and κ is the curvature. In the context of electronic

structure calculations like DFT, the radial polarization can be expressed as:⁵⁰

$$p_r = \frac{1}{A} \int_{\Omega} (r - R_{\text{eff}}) \rho(\mathbf{x}) d\mathbf{x}, \quad (2)$$

where A is the cross-sectional area of the deformed sheet within the domain Ω , r is the radial coordinate of the spatial point \mathbf{x} , R_{eff} is the *radial centroid* of the ions, and $\rho(\mathbf{x})$ is the electron density. Note that the *radial dipole moment* has been normalized using the area rather than the volume, as is common practice, given the significant disagreement associated with the thickness of atomic monolayers.⁶⁷

We calculate the flexoelectric coefficient by using a numerical approximation for the derivative in Eq. 1, the alternative being the more involved DFPT-based approaches, for which a symmetry-adapted variant at finite deformations is yet to be developed. Specifically, we compute the radial polarization at multiple curvatures in the vicinity of the curvature at which the flexoelectric coefficient is desired and determine the slope from a curve fit to the data. In particular, as illustrated in Fig. 1, edge-related effects are removed by mapping the bent structure periodically in the angular direction, and the cyclic symmetry of the resultant structure is then exploited to perform highly efficient Kohn-Sham calculations^{68–70} for the structural and electronic ground state using the Cyclix DFT code⁶⁸ — large-scale parallel implementation of cyclic+helical symmetry in state-of-the-art real-space DFT code SPARC.^{71,72}

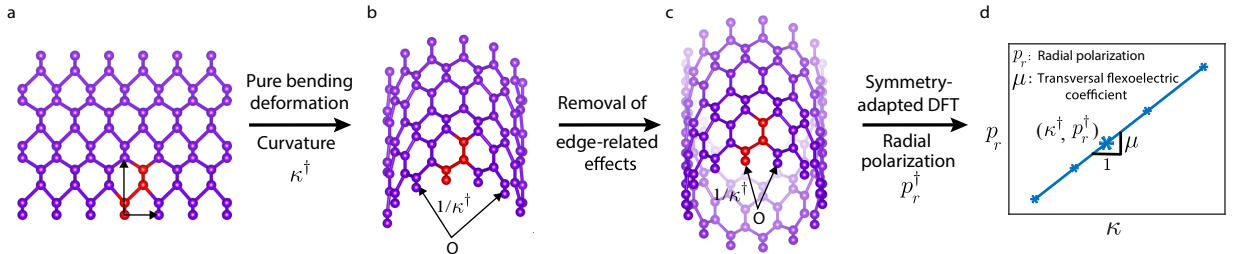


Figure 1: Schematic illustrating the calculation of transversal flexoelectric coefficient for atomic monolayers using symmetry-adapted DFT simulations.^{50,68,69} The atoms in the unit cell are colored red.

We use the aforescribed framework to calculate transversal flexoelectric coefficients for fifty select atomic monolayers along their principal directions. Specifically, we consider bending curvatures in the range of $0.14 < \kappa < 0.24 \text{ nm}^{-1}$ — resulting system sizes are intractable to traditional DFT implementations — commensurate with those found in experiments.^{63–66} We select representative honeycomb lattice materials from each of Groups IV, III-V, V monolayers, TMDs, and Group III monochalcogenides, as well as rectangular lattice materials from each of Group V monolayers, Group IV monochalcogenides, TMTs, and Group V chalcogenides. The choice of these groups is motivated by the significant success in the synthesis of affiliated monolayers, which are found to demonstrate interesting and novel properties.^{31–35,73–75}

In all simulations, we employ the Perdew-Burke-Ernzerhof (PBE)⁷⁶ variant of the generalized gradient approximation (GGA) for the exchange-correlation functional and optimized norm-conserving Vanderbilt (ONCV) pseudopotentials⁷⁷ from the SG15 collection.⁷⁸ All numerical parameters, including grid spacing, k-point sampling for Brillouin zone integration, vacuum in radial direction, and structural (cell and atom) relaxation tolerances are chosen such that the computed flexoelectric coefficients are accurate to within $0.005 e$, as verified through convergence studies (Supplementary Material). This translates to the requirement of the ground state energy being converged to within 10^{-5} Ha/atom. Note that the coefficients predicted here are expected to be reasonably robust against the two main approximations within DFT, i.e., pseudopotential and exchange-correlation functional, as discussed next.

The equilibrium geometries for the flat monolayers computed using ABINIT⁷⁹ (Supplementary Material) are in good agreement with previous theoretical predictions^{37,38} and experimental measurements.^{31–35,73,74} Furthermore, the normalized difference in electron density between the PBE GGA and HSE hybrid functional⁸⁰ for the undeformed configurations is $\mathcal{O}(1 - 2)$, comparable to the agreement between hybrid functionals and the gold standard Coupled Cluster Singles and Doubles (CCSD) method.⁸¹ Similar differences are observed when spin orbit coupling is included. Since the flexoelectric coefficient is dependent on

electron density differences from the flat configuration, which corresponds to small (linear) perturbations in the current context, significant error cancellations are expected. This is evidenced by recent work where both local and semilocal functionals predict nearly identical coefficients for group IV monolayers.⁵⁰

Table 1: Transversal flexoelectric coefficient along principal directions for the fifty select atomic monolayers from first principles DFT calculations.

Group	Material	Flexoelectric coefficient (e)		Group	Material	Flexoelectric coefficient (e)	
		μ_1	μ_2			μ_1	μ_2
Groups IV, III-V monolayers (h1)	Si	0.19	0.19	Group III monochalcogenides (h3)	GaS	0.48	0.48
	BN	0.20	0.20		GaSe	0.48	0.50
	C	0.22	0.22		InS	0.47	0.47
	Sn	0.26	0.25		InSe	0.49	0.48
	Ge	0.27	0.27		InTe	0.59	0.54
Group V monolayers (h1)	P	0.25	0.25		GaTe	0.60	0.59
	As	0.26	0.27	Group V monolayers (t1)	P	0.31	0.33
	Bi	0.33	0.33		As	0.31	0.31
	Sb	0.34	0.34		Bi	0.51	0.51
Transition metal dichalcogenides (h2)	ZrS ₂	0.45	0.45		Sb	0.54	0.54
	TiS ₂	0.45	0.45	Group IV monochalcogenides (t1)	GeSe	0.38	0.39
	ZrSe ₂	0.46	0.47		GeS	0.42	0.41
	TiSe ₂	0.41	0.40		SnSe	0.41	0.41
	NbS ₂	0.51	0.52		SnS	0.42	0.40
	NbSe ₂	0.51	0.54	Transition metal trichalcogenides (t2)	ZrS ₃	0.66	0.64
	HfS ₂	0.57	0.56		TiS ₃	0.67	0.63
	ZrTe ₂	0.55	0.54		ZrSe ₃	0.68	0.66
	TiTe ₂	0.58	0.56		HfS ₃	0.80	0.78
	MoSe ₂	0.57	0.57		HfSe ₃	0.81	0.78
	MoS ₂	0.57	0.58		ZrTe ₃	0.98	0.86
	WS ₂	0.59	0.59	Group V chalcogenides (t3)	P ₂ S ₃	0.24	0.25
	WSe ₂	0.59	0.58		P ₂ Se ₃	0.25	0.26
	NbTe ₂	0.64	0.67		As ₂ S ₃	0.27	0.28
MoTe ₂	0.71	0.72	As ₂ Se ₃		0.28	0.30	
WTe ₂	0.73	0.74	As ₂ Te ₃		0.38	0.39	

In Table 1, we present the computed transversal flexoelectric coefficients for the chosen atomic monolayers along their principal directions, which is summarized visually in Fig. 2. The variables μ_1 and μ_2 are used to represent the flexoelectric coefficient values along the x_1 and x_2 directions, respectively, whose orientation relative to the different lattice structures can be seen in Fig. 3. For honeycomb lattices, these correspond to the zigzag and armchair

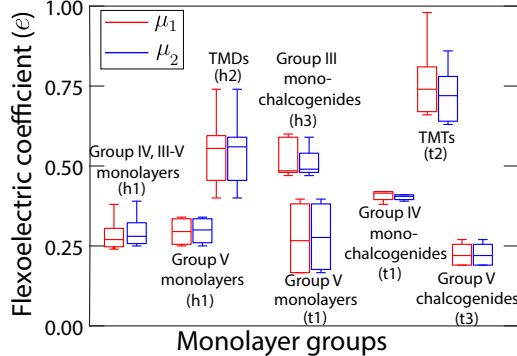


Figure 2: Transversal flexoelectric coefficients for the select atomic monolayer groups.

directions, respectively. A single value is listed in all cases since the flexoelectric coefficients are essentially constant for the bending curvatures considered here (Supplementary Material), signaling linear response for the monolayers in this regime. Note that depending on the application of interest, the flexoelectric coefficient that relates polarization to bending moment might be more informative. Therefore, the values for the so defined flexoelectric coefficient have been provided in the Supplementary Material, for which we use the bending moduli from previous work for forty-four of the materials,²⁴ with the remaining calculated here (Supplementary Material).

The flexoelectric coefficients span a wide range of values from $0.19 - 0.98 e$, with silicene and ZrTe_3 being at the bottom and top ends of the spectrum, respectively, and graphene towards the lower end with $0.22 e$. In terms of the classification, Groups IV, III-V monolayers and TMTs have the smallest and largest coefficients, respectively. Interestingly, we find that the flexoelectric coefficients are similar along both principal directions, irrespective of the lattice structure. Though this is to be expected for honeycomb lattices, which usually demonstrate isotropic behavior/properties,^{24,82-84} it is most unusual for rectangular lattices, where the behavior/properties tend to be highly anisotropic.^{24,85-88} This is not a consequence of relaxation-related effects — cause for the bending moduli of some rectangular lattices to be isotropic²⁴ — which are minor in the current context (Supplementary Material). Note that when the flexoelectric coefficient relating the polarization to the bending moment is considered (Supplementary Material), the values span more than two orders of magnitude, with the

trends essentially reversed, i.e., Groups IV, III-V monolayers and TMTs now have the largest and smallest coefficients, respectively. In particular, stanene has the largest value, given its extremely small bending moduli,²⁴ and ZrTe_3 has the smallest value, given its extremely large bending moduli.²⁴ Also, the coefficients for the rectangular lattices differ significantly in the principal directions, given their significant anisotropy in bending moduli.²⁴

In comparisons with experiments, while there is relatively good agreement for MoS_2 (difference of $\sim 0.09 e^{43}$), there is some disagreement for MoSe_2 , WS_2 , and WSe_2 (differences of up to $\sim 0.48 e^{44}$). These differences can be attributed to the use of a substrate, and the substantial error bars ($\sim 0.18 e$) associated with the measurements. In comparisons to DFT-based results, the values for graphene predicted previously^{47,48,51} are more than a factor of two smaller than those here. This can be attributed to the use of an ill defined flexoelectric coefficient⁴⁸ and an artificial partitioning of the electron density,^{47,51} as discussed in previous work.⁵⁰ The values reported previously for TMDs⁴⁹ (MX_2 : $\text{M}=\text{Mo}, \text{W}$; $\text{X}=\text{S}, \text{Se}, \text{Te}$) are up two orders of magnitude smaller than those here, a consequence of using an ill defined flexoelectric coefficient and a wrinkled sheet geometry that has non-uniform strain gradients. Similarly small values for a few monolayers have been predicted very recently,⁶⁰ which can be attributed to the difference in the definition of the flexoelectric coefficient.

To get further insight into the results, considering representative materials from each group, we plot in Fig. 3 contours of electron density difference between the flat and bent monolayers for bending along the x_2 direction. We also present the charge transfer due to bending as determined via Bader analysis.⁸⁹ Similar results for bending along the x_1 direction can be found in the Supplementary Material. Three key observations can be made from these figures. First, charge transfer occurs from the compressive side to tensile side of the neutral axis, indicating that the origin of the flexoelectric effect for monolayers is electronic rather than ionic. The charge transfer is similar for both bending directions, resulting in similar flexoelectric coefficients. Second, the electron density perturbations are localized near the nuclei, resulting in atomic dipoles that accumulate to generate the total

radial dipole moment. The strength of these dipoles is dependent on the atom's polarizability, as evidenced from the significantly larger charge transfer for Te compared to S and Se in the tungsten dichalcogenides. Indeed, polarizability of S and Se are similar, both of which are significantly smaller than Te.⁹⁰ Third, the atomic polarization (i.e., atomic dipole per unit area) increases with distance from neutral axis, as evidenced for the S atom in the various monolayers. This can be attributed to the increase in stress with neutral axis distance.

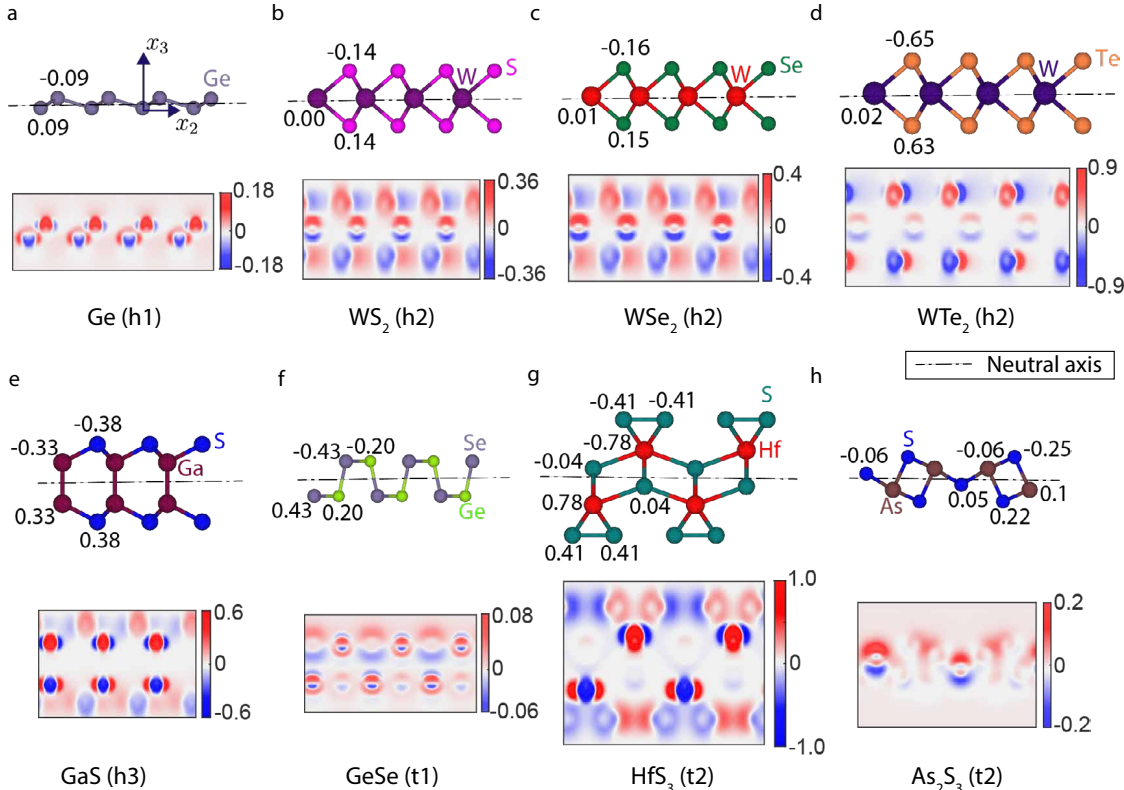


Figure 3: Contours of electron density difference (integrated along the x_1 direction) between the flat and bent ($\kappa \sim 0.2 \text{ nm}^{-1}$) atomic monolayers. The contours are plotted on the x_2x_3 -plane in the undeformed configuration. The charge transfer due to bending, which is shown near the corresponding atoms in the lattice structure, is obtained from Bader analysis.⁸⁹

The above observations suggest the flexoelectric coefficients for the monolayers is primarily determined by their thickness, elastic modulus along bending direction, and sum of polarizabilities of constituent atoms. The dependence on atom polarizabilities is in agreement with literature,^{91,92} where it has been proposed that the flexoelectric coefficient is proportional to the dielectric permittivity, which can be related to the atom polarizabilities

through the Clausius–Mossotti relation.⁹³ Using the three features listed above, we perform a third order polynomial regression for the flexoelectric coefficients, the results of which are presented in Fig. 4. Note that the thickness has been defined to be the distance between the two atoms furthest from the neutral axis plus an additional 12 Bohr (results insensitive to this choice). The fit is very good, suggesting that the flexoelectric coefficients for atomic monolayers are primarily decided by the three aforementioned features. We also perform a linear regression between the computed coefficients and each of the features independently, the results of which are presented in Fig. 4. The fits are good, suggesting that the flexoelectric coefficient generally increases with monolayer thickness, elastic modulus along bending direction, and sum of polarizability of constituent atoms.

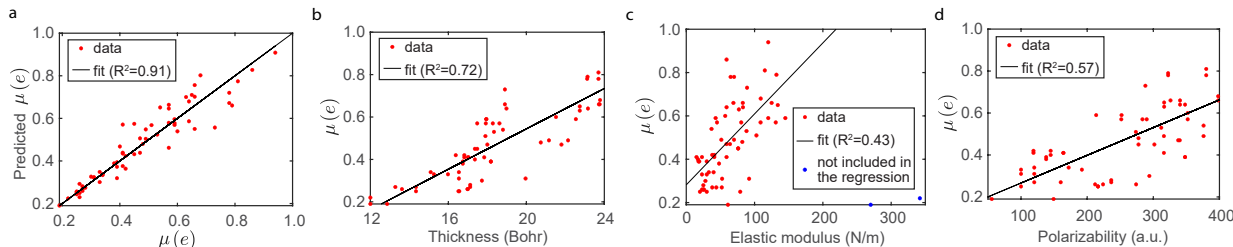


Figure 4: (a) Set of calculated transversal flexoelectric coefficients and its third order polynomial regression with the features being thickness, elastic modulus along bending direction, and sum of polarizability of constituent atoms. (b), (c), and (d) Set of computed flexoelectric coefficients and its linear regression with the feature being thickness, elastic modulus along bending direction, and sum of polarizability of constituent atoms, respectively. In all plots, R^2 denotes the coefficient of determination for the regression.

In summary, we have calculated transversal flexoelectric coefficients along the principal directions for fifty select atomic monolayers using ab initio DFT. Specifically, considering representative materials from each of the prominent monolayer groups, we have determined the coefficients at practically relevant bending curvatures using symmetry-adapted DFT calculations. We have found that the monolayers demonstrate linear behavior and have similar flexoelectric coefficients along both principal directions, with values for TMTs being up to a factor of five larger than graphene. In addition, we have found electronic origins for the flexoelectric effect, which increases with monolayer thickness, elastic modulus along bending

direction, and sum of polarizability of constituent atoms. Overall, this work provides an important reference for the transversal flexoelectric coefficients for a number of important atomic monolayers, and provides fundamental insights into the underlying mechanisms. The flexoelectric coefficients predicted here could prove useful in the design of nanoelectromechanical devices, with the regression model serving as a powerful tool for preliminary searches through large databases of two-dimensional materials.

Acknowledgments

S.K. and P.S. gratefully acknowledge the support of the U.S. National Science Foundation (CAREER-1553212 and MRI-1828187). D.C. and I.A. acknowledge the support of the Generalitat de Catalunya (ICREA Academia award for excellence in research to I.A., and Grant No. 2017-SGR-1278), and the European Research Council (StG-679451 to I.A.). CIMNE is recipient of a Severo Ochoa Award of Excellence from the MINECO.

Supporting Information Available

Equilibrium geometry for the atomic monolayers, Unrelaxed transversal flexoelectric coefficients, Radial polarization vs. curvature data, Convergence study for the computed flexoelectric coefficients, Flexoelectric coefficient relating polarization to bending moment, Bader analysis results for bending along the x_1 -direction, Bending moduli for select monolayers

Conflicts of interest

There are no conflicts to declare.

References

- (1) Tagantsev, A. K. Electric polarization in crystals and its response to thermal and elastic perturbations. *Phase Transit.* **1991**, *35*, 119–203.
- (2) Yudin, P.; Tagantsev, A. Fundamentals of flexoelectricity in solids. *Nanotechnology* **2013**, *24*, 432001.
- (3) Zubko, P.; Catalan, G.; Tagantsev, A. K. Flexoelectric effect in solids. *Annu. Rev. Mater. Sci.* **2013**, *43*.
- (4) Nguyen, T. D.; Mao, S.; Yeh, Y.-W.; Purohit, P. K.; McAlpine, M. C. Nanoscale flexoelectricity. *Advanced Materials* **2013**, *25*, 946–974.
- (5) Ahmadpoor, F.; Sharma, P. Flexoelectricity in two-dimensional crystalline and biological membranes. *Nanoscale* **2015**, *7*, 16555–16570.
- (6) Narvaez, J.; Vasquez-Sancho, F.; Catalan, G. Enhanced flexoelectric-like response in oxide semiconductors. *Nature* **2016**, *538*, 219–221.
- (7) Krichen, S.; Sharma, P. Flexoelectricity: a perspective on an unusual electromechanical coupling. *J. Appl. Mech.* **2016**, *83*.
- (8) Wang, B.; Gu, Y.; Zhang, S.; Chen, L.-Q. Flexoelectricity in solids: Progress, challenges, and perspectives. *Prog. Mater. Sci.* **2019**, *106*, 100570.
- (9) Hill, E. W.; Vijayaraghavan, A.; Novoselov, K. Graphene sensors. *IEEE Sensors Journal* **2011**, *11*, 3161–3170.
- (10) Wang, Q.-M.; Du, X.-H.; Xu, B.; Cross, L. E. Electromechanical coupling and output efficiency of piezoelectric bending actuators. *IEEE transactions on ultrasonics, ferroelectrics, and frequency control* **1999**, *46*, 638–646.

- (11) Xu, S.; Qin, Y.; Xu, C.; Wei, Y.; Yang, R.; Wang, Z. L. Self-powered nanowire devices. *Nature nanotechnology* **2010**, *5*, 366–373.
- (12) Wang, X.; Tian, H.; Xie, W.; Shu, Y.; Mi, W.-T.; Mohammad, M. A.; Xie, Q.-Y.; Yang, Y.; Xu, J.-B.; Ren, T.-L. Observation of a giant two-dimensional band-piezoelectric effect on biaxial-strained graphene. *NPG Asia Materials* **2015**, *7*, e154–e154.
- (13) da Cunha Rodrigues, G.; Zelenovskiy, P.; Romanyuk, K.; Luchkin, S.; Kopelevich, Y.; Kholkin, A. Strong piezoelectricity in single-layer graphene deposited on SiO₂ grating substrates. *Nature communications* **2015**, *6*, 1–6.
- (14) Pu, J.; Yomogida, Y.; Liu, K.-K.; Li, L.-J.; Iwasa, Y.; Takenobu, T. Highly flexible MoS₂ thin-film transistors with ion gel dielectrics. *Nano Letters* **2012**, *12*, 4013–4017.
- (15) Lee, G.-H.; Yu, Y.-J.; Cui, X.; Petrone, N.; Lee, C.-H.; Choi, M. S.; Lee, D.-Y.; Lee, C.; Yoo, W. J.; Watanabe, K. et al. Flexible and transparent MoS₂ field-effect transistors on hexagonal boron nitride-graphene heterostructures. *ACS Nano* **2013**, *7*, 7931–7936.
- (16) Salvatore, G. A.; Munzenrieder, N.; Barraud, C.; Petti, L.; Zysset, C.; Buthe, L.; Ensslin, K.; Troster, G. Fabrication and transfer of flexible few-layers MoS₂ thin film transistors to any arbitrary substrate. *ACS Nano* **2013**, *7*, 8809–8815.
- (17) Yoon, J.; Park, W.; Bae, G.-Y.; Kim, Y.; SooJang, H.; Hyun, Y.; Lim, S. K.; Kahng, Y. H.; Hong, W.-K.; Lee, B. H. et al. Highly flexible and transparent multilayer MoS₂ transistors with graphene electrodes. *Small* **2013**, *9*, 3295–3300.
- (18) Zhang, Y.; Zheng, B.; Zhu, C.; Zhang, X.; Tan, C.; Li, H.; Chen, B.; Yang, J.; Chen, J.; Huang, Y. et al. Single-layer transition metal dichalcogenide nanosheet-based nanosensors for rapid, sensitive, and multiplexed detection of DNA. *Advanced Materials* **2015**, *27*, 935–939.

- (19) Sakhaee-Pour, A.; Ahmadian, M.; Vafai, A. Potential application of single-layered graphene sheet as strain sensor. *Solid State Communications* **2008**, *147*, 336–340.
- (20) Sazonova, V.; Yaish, Y.; Üstünel, H.; Roundy, D.; Arias, T. A.; McEuen, P. L. A tunable carbon nanotube electromechanical oscillator. *Nature* **2004**, *431*, 284.
- (21) Bunch, J. S.; Zande, A. M. V. D.; Verbridge, S. S.; Frank, I. W.; Tanenbaum, D. M.; Parpia, J. M.; Craighead, H. G.; McEuen, P. L. Electromechanical resonators from graphene sheets. *Science* **2007**, *315*, 490–493.
- (22) Novoselov, K.; Neto, A. C. Two-dimensional crystals-based heterostructures: materials with tailored properties. *Physica Scripta* **2012**, *2012*, 014006.
- (23) Qin, Y.; Peng, Q.; Ding, Y.; Lin, Z.; Wang, C.; Li, Y.; Xu, F.; Li, J.; Yuan, Y.; He, X. et al. Lightweight, superelastic, and mechanically flexible graphene/polyimide nanocomposite foam for strain sensor application. *ACS Nano* **2015**, *9*, 8933–8941.
- (24) Kumar, S.; Suryanarayana, P. Bending moduli for forty-four select atomic monolayers from first principles. *Nanotechnology* **2020**, *31*, 43LT01.
- (25) Bhaskar, U. K.; Banerjee, N.; Abdollahi, A.; Solanas, E.; Rijnders, G.; Catalan, G. Flexoelectric MEMS: towards an electromechanical strain diode. *Nanoscale* **2016**, *8*, 1293–1298.
- (26) Abdollahi, A.; Arias, I. Constructive and Destructive Interplay Between Piezoelectricity and Flexoelectricity in Flexural Sensors and Actuators. *Journal of Applied Mechanics* **2015**, *82*, 121003(1–4).
- (27) Abdollahi, A.; Domingo, N.; Arias, I.; Catalan, G. Converse flexoelectricity yields large piezoresponse force microscopy signals in non-piezoelectric materials. *Nature Communications* **2019**, *10*, 1266.

- (28) Mas-Balleste, R.; Gomez-Navarro, C.; Gomez-Herrero, J.; Zamora, F. 2D materials: to graphene and beyond. *Nanoscale* **2011**, *3*, 20–30.
- (29) Butler, S. Z.; Hollen, S. M.; Cao, L.; Cui, Y.; Gupta, J. A.; Gutiérrez, H. R.; Heinz, T. F.; Hong, S. S.; Huang, J.; Ismach, A. F. et al. Progress, Challenges, and Opportunities in Two-Dimensional Materials Beyond Graphene. *ACS Nano* **2013**, *7*, 2898–2926.
- (30) Geng, D.; Yang, H. Y. Recent advances in growth of novel 2D materials: beyond graphene and transition metal dichalcogenides. *Advanced Materials* **2018**, *30*, 1800865.
- (31) Balendhran, S.; Walia, S.; Nili, H.; Sriram, S.; Bhaskaran, M. Elemental analogues of graphene: silicene, germanene, stanene, and phosphorene. *Small* **2015**, *11*, 640–652.
- (32) Zhou, S.; Liu, C.-C.; Zhao, J.; Yao, Y. Monolayer group-III monochalcogenides by oxygen functionalization: a promising class of two-dimensional topological insulators. *npj Quantum Materials* **2018**, *3*, 1–7.
- (33) Vaughn, D. D.; Patel, R. J.; Hickner, M. A.; Schaak, R. E. Single-crystal colloidal nanosheets of GeS and GeSe. *Journal of the American Chemical Society* **2010**, *132*, 15170–15172.
- (34) Zhang, S.; Guo, S.; Chen, Z.; Wang, Y.; Gao, H.; Gómez-Herrero, J.; Ares, P.; Zamora, F.; Zhu, Z.; Zeng, H. Recent progress in 2D group-VA semiconductors: from theory to experiment. *Chemical Society Reviews* **2018**, *47*, 982–1021.
- (35) Dai, J.; Li, M.; Zeng, X. C. Group IVB transition metal trichalcogenides: a new class of 2D layered materials beyond graphene. *Wiley Interdisciplinary Reviews: Computational Molecular Science* **2016**, *6*, 211–222.
- (36) Wang, C.; Zheng, C.; Gao, G. Bulk and monolayer ZrS₃ as promising anisotropic ther-

- moelectric materials: A comparative study. *The Journal of Physical Chemistry C* **2020**, *124*, 6536–6543.
- (37) Hastrup, S.; Strange, M.; Pandey, M.; Deilmann, T.; Schmidt, P. S.; Hinsche, N. F.; Gjerding, M. N.; Torelli, D.; Larsen, P. M.; Riis-Jensen, A. C. et al. The Computational 2D Materials Database: high-throughput modeling and discovery of atomically thin crystals. *2D Materials* **2018**, *5*, 042002.
- (38) Zhou, J.; Shen, L.; Costa, M. D.; Persson, K. A.; Ong, S. P.; Huck, P.; Lu, Y.; Ma, X.; Chen, Y.; Tang, H. et al. 2DMatPedia, an open computational database of two-dimensional materials from top-down and bottom-up approaches. *Scientific data* **2019**, *6*, 1–10.
- (39) Kerszberg, N.; Suryanarayana, P. Ab initio strain engineering of graphene: opening bandgaps up to 1 eV. *RSC Advances* **2015**, *5*, 43810–43814.
- (40) Fei, R.; Li, W.; Li, J.; Yang, L. Giant piezoelectricity of monolayer group IV monochalcogenides: SnSe, SnS, GeSe, and GeS. *Applied Physics Letters* **2015**, *107*, 173104.
- (41) Hsu, Y.-T.; Vaezi, A.; Fischer, M. H.; Kim, E.-A. Topological superconductivity in monolayer transition metal dichalcogenides. *Nature communications* **2017**, *8*, 1–6.
- (42) Jiang, X.-F.; Weng, Q.; Wang, X.-B.; Li, X.; Zhang, J.; Golberg, D.; Bando, Y. Recent progress on fabrications and applications of boron nitride nanomaterials: a review. *Journal of Materials Science & Technology* **2015**, *31*, 589–598.
- (43) Brennan, C. J.; Ghosh, R.; Koul, K.; Banerjee, S. K.; Lu, N.; Yu, E. T. Out-of-plane electromechanical response of monolayer molybdenum disulfide measured by piezoresponse force microscopy. *Nano Letters* **2017**, *17*, 5464–5471.

- (44) Brennan, C. J.; Koul, K.; Lu, N.; Yu, E. T. Out-of-plane electromechanical coupling in transition metal dichalcogenides. *Applied Physics Letters* **2020**, *116*, 053101.
- (45) Hohenberg, P.; Kohn, W. Inhomogeneous Electron Gas. *Physical Review* **1964**, *136*, B864–B871.
- (46) Kohn, W.; Sham, L. J. Self-Consistent Equations Including Exchange and Correlation Effects. *Physical Review* **1965**, *140*, A1133–A1138.
- (47) Dumitrică, T.; Landis, C. M.; Yakobson, B. I. Curvature-induced polarization in carbon nanoshells. *Chemical physics letters* **2002**, *360*, 182–188.
- (48) Kalinin, S. V.; Meunier, V. Electronic flexoelectricity in low-dimensional systems. *Physical Review B* **2008**, *77*, 033403.
- (49) Shi, W.; Guo, Y.; Zhang, Z.; Guo, W. Flexoelectricity in monolayer transition metal dichalcogenides. *The journal of physical chemistry letters* **2018**, *9*, 6841–6846.
- (50) Codony, D.; Arias, I.; Suryanarayana, P. Transversal flexoelectric coefficient for nanostructures at finite deformations from first principles. *arXiv preprint arXiv:2010.01747* **2020**,
- (51) Kvashnin, A. G.; Sorokin, P. B.; Yakobson, B. I. Flexoelectricity in carbon nanostructures: nanotubes, fullerenes, and nanocones. *The journal of physical chemistry letters* **2015**, *6*, 2740–2744.
- (52) Gonze, X.; Lee, C. Dynamical matrices, Born effective charges, dielectric permittivity tensors, and interatomic force constants from density-functional perturbation theory. *Phys. Rev. B* **1997**, *55*, 10355.
- (53) Baroni, S.; De Gironcoli, S.; Dal Corso, A.; Giannozzi, P. Phonons and related crystal properties from density-functional perturbation theory. *Rev. Mod. Phys.* **2001**, *73*, 515.

- (54) Hong, J.; Vanderbilt, D. First-principles theory of frozen-ion flexoelectricity. *Physical Review B* **2011**, *84*, 180101.
- (55) Hong, J.; Vanderbilt, D. First-principles theory and calculation of flexoelectricity. *Phys. Rev. B* **2013**, *88*, 174107.
- (56) Stengel, M. Flexoelectricity from density-functional perturbation theory. *Phys. Rev. B* **2013**, *88*, 174106.
- (57) Stengel, M. Surface control of flexoelectricity. *Phys. Rev. B* **2014**, *90*, 201112(R).
- (58) Dreyer, C. E.; Stengel, M.; Vanderbilt, D. Current-density implementation for calculating flexoelectric coefficients. *Phys. Rev. B* **2018**, *98*, 075153.
- (59) Royo, M.; Stengel, M. First-principles theory of spatial dispersion: Dynamical quadrupoles and flexoelectricity. *Physical Review X* **2019**, *9*, 021050.
- (60) Springolo, M.; Royo, M.; Stengel, M. Flexoelectricity in two-dimensional materials. *arXiv preprint arXiv:2010.08470* **2020**,
- (61) Javvaji, B.; He, B.; Zhuang, X.; Park, H. S. High flexoelectric constants in Janus transition-metal dichalcogenides. *Physical Review Materials* **2019**, *3*, 125402.
- (62) Zhuang, X.; He, B.; Javvaji, B.; Park, H. S. Intrinsic bending flexoelectric constants in two-dimensional materials. *Physical Review B* **2019**, *99*, 054105.
- (63) Lindahl, N.; Midtvedt, D.; Svensson, J.; Nerushev, O. A.; Lindvall, N.; Isacson, A.; Campbell, E. E. Determination of the bending rigidity of graphene via electrostatic actuation of buckled membranes. *Nano Letters* **2012**, *12*, 3526–3531.
- (64) Han, E.; Yu, J.; Annevelink, E.; Son, J.; Kang, D. A.; Watanabe, K.; Taniguchi, T.; Ertekin, E.; Huang, P. Y.; van der Zande, A. M. Ultrasoft slip-mediated bending in few-layer graphene. *Nature materials* **2019**, 1–5.

- (65) Wang, G.; Dai, Z.; Xiao, J.; Feng, S.; Weng, C.; Liu, L.; Xu, Z.; Huang, R.; Zhang, Z. Bending of Multilayer van der Waals Materials. *Physical Review Letters* **2019**, *123*, 116101.
- (66) Qu, W.; Bagchi, S.; Chen, X.; Chew, H. B.; Ke, C. Bending and interlayer shear moduli of ultrathin boron nitride nanosheet. *Journal of Physics D: Applied Physics* **2019**, *52*, 465301.
- (67) Huang, Y.; Wu, J.; Hwang, K.-C. Thickness of graphene and single-wall carbon nanotubes. *Physical review B* **2006**, *74*, 245413.
- (68) Sharma, A.; Suryanarayana, P. Cyclic+helical symmetry-adapted real-space density functional theory: Application to torsional deformation of carbon nanotubes. **2020**,
- (69) Ghosh, S.; Banerjee, A. S.; Suryanarayana, P. Symmetry-adapted real-space density functional theory for cylindrical geometries: Application to large group-IV nanotubes. *Physical Review B* **2019**, *100*, 125143.
- (70) Banerjee, A. S.; Suryanarayana, P. Cyclic density functional theory: A route to the first principles simulation of bending in nanostructures. *Journal of the Mechanics and Physics of Solids* **2016**, *96*, 605–631.
- (71) Xu, Q.; Sharma, A.; Comer, B.; Huang, H.; Chow, E.; Medford, A. J.; Pask, J. E.; Suryanarayana, P. SPARC: Simulation Package for Ab-initio Real-space Calculations. *arXiv preprint arXiv:2005.10431* **2020**,
- (72) Ghosh, S.; Suryanarayana, P. SPARC: Accurate and efficient finite-difference formulation and parallel implementation of Density Functional Theory: Extended systems. *Computer Physics Communications* **2017**, *216*, 109–125.
- (73) Coleman, J. N.; Lotya, M.; O'Neill, A.; Bergin, S. D.; King, P. J.; Khan, U.; Young, K.;

- Gaucher, A.; De, S.; Smith, R. J. et al. Two-dimensional nanosheets produced by liquid exfoliation of layered materials. *Science* **2011**, *331*, 568–571.
- (74) Novoselov, K. S.; Jiang, D.; Schedin, F.; Booth, T. J.; Khotkevich, V. V.; Morozov, S. V.; Geim, A. K. Two-dimensional atomic crystals. *Proceedings of the National Academy of Sciences* **2005**, *102*, 10451–10453.
- (75) Šiškins, M.; Lee, M.; Alijani, F.; van Blankenstein, M. R.; Davidovikj, D.; van der Zant, H. S.; Steeneken, P. G. Highly anisotropic mechanical and optical properties of 2D layered As_2S_3 membranes. *ACS nano* **2019**, *13*, 10845–10851.
- (76) Perdew, J. P.; Yue, W. Accurate and simple density functional for the electronic exchange energy: Generalized gradient approximation. *Physical Review B* **1986**, *33*, 8800.
- (77) Hamann, D. R. Optimized norm-conserving Vanderbilt pseudopotentials. *Physical Review B* **2013**, *88*, 085117.
- (78) Schlipf, M.; Gygi, F. Optimization algorithm for the generation of ONCV pseudopotentials. *Computer Physics Communications* **2015**, *196*, 36 – 44.
- (79) Gonze, X.; Beuken, J. M.; Caracas, R.; Detraux, F.; Fuchs, M.; Rignanese, G. M.; Sindic, L.; Verstraete, M.; Zerah, G.; Jollet, F. et al. First-principles computation of material properties: the ABINIT software project. *Computational Materials Science* **2002**, *25*, 478–492(15).
- (80) Heyd, J.; Scuseria, G. E.; Ernzerhof, M. Hybrid functionals based on a screened Coulomb potential. *The Journal of chemical physics* **2003**, *118*, 8207–8215.
- (81) Medvedev, M. G.; Bushmarinov, I. S.; Sun, J.; Perdew, J. P.; Lyssenko, K. A. Density functional theory is straying from the path toward the exact functional. *Science* **2017**, *355*, 49–52.

- (82) Ding, H.; Zhen, Z.; Imtiaz, H.; Guo, W.; Zhu, H.; Liu, B. Why are most 2D lattices hexagonal? The stability of 2D lattices predicted by a simple mechanics model. *Extreme Mechanics Letters* **2019**, *32*, 100507.
- (83) Rasmussen, F. A.; Thygesen, K. S. Computational 2D materials database: electronic structure of transition-metal dichalcogenides and oxides. *The Journal of Physical Chemistry C* **2015**, *119*, 13169–13183.
- (84) Li, W.; Li, J. Piezoelectricity in two-dimensional group-III monochalcogenides. *Nano Research* **2015**, *8*, 3796–3802.
- (85) Li, L.; Han, W.; Pi, L.; Niu, P.; Han, J.; Wang, C.; Su, B.; Li, H.; Xiong, J.; Bando, Y. et al. Emerging in-plane anisotropic two-dimensional materials. *InfoMat* **2019**, *1*, 54–73.
- (86) Xia, F.; Wang, H.; Jia, Y. Rediscovering black phosphorus as an anisotropic layered material for optoelectronics and electronics. *Nature Communications* **2014**, *5*, 1–6.
- (87) Wang, X.; Jones, A. M.; Seyler, K. L.; Tran, V.; Jia, Y.; Zhao, H.; Wang, H.; Yang, L.; Xu, X.; Xia, F. Highly anisotropic and robust excitons in monolayer black phosphorus. *Nature Nanotechnology* **2015**, *10*, 517–521.
- (88) Luo, Z.; Maassen, J.; Deng, Y.; Du, Y.; Garrelts, R. P.; Lundstrom, M. S.; Peide, D. Y.; Xu, X. Anisotropic in-plane thermal conductivity observed in few-layer black phosphorus. *Nature Communications* **2015**, *6*, 1–8.
- (89) Bader, R.; Nguyen-Dang, T. *Advances in Quantum Chemistry*; Elsevier, 1981; Vol. 14; pp 63–124.
- (90) Tandon, H.; Chakraborty, T.; Suhag, V. A new scale of atomic static dipole polarizability invoking other periodic descriptors. *Journal of Mathematical Chemistry* **2019**, *57*, 2142–2153.

- (91) Tagantsev, A. Theory of flexoelectric effect in crystals. *Zhurnal Eksperimental'noi i Teoreticheskoi Fiziki* **1985**, 88, 2108–22.
- (92) Ma, L. L.; Chen, W. J.; Zheng, Y. In *Handbook of Mechanics of Materials*; Schmauder, S., Chen, C.-S., Chawla, K. K., Chawla, N., Chen, W., Kagawa, Y., Eds.; Springer Singapore: Singapore, 2019; pp 549–589.
- (93) Griffiths, D. J. *Introduction to Electrodynamics*, 4th ed.; Cambridge University Press, 2017.